

The “benzyl alcohol route”: An elegant approach towards doped and multimetal oxide nanocrystals

Short review and ZnAl_2O_4 nanostructures by oriented attachment

Nicola Pinna · Mohamed Karmaoui ·
Marc-Georg Willinger

Received: 9 September 2009 / Accepted: 4 November 2009 / Published online: 13 January 2010
© Springer Science+Business Media, LLC 2009

Abstract In this article, the versatility and the potential of the “benzyl alcohol route” for the synthesis of multimetal and doped metal oxides are highlighted in the first part of the manuscript. Among the presented examples, some materials have not been accessible by other solution syntheses and could so far only be obtained through solid state reactions. The second part describes the synthesis and characterization of 5–6 nm ZnAl_2O_4 nanoparticles which form flower-like aggregates through the oriented attachment crystallization mechanism.

Keywords Nanocrystals · Metal oxides · Nonaqueous synthesis

1 Introduction

Various liquid phase chemical approaches have been introduced in the past decades for the synthesis of metal oxide nanoparticles [9, 15, 21, 32, 43]. They were reported extremely successful for the production of simple oxides (e.g. binary). Indeed, dozens of routes for the production of titanium and zinc oxide nanoparticles can be found in the recent literature. In contrast, approaches leading to the

formation of multimetal and doped metal oxides by soft chemistry approaches are rarely reported and many oxides can still only be obtained through solid state reactions. The main reason resides in the difficulty to match the reactivity of the different metal precursors in solution, which prevents the formation of multimetal phases or the homogeneous doping of simple oxides [43]. This is especially true for aqueous routes (e.g. sol-gel) since the hydrolysis rates are generally fast and strongly depend on the metal center [18]. To circumvent this problem, numerous studies were conducted in the aim of modifying the metal complexes, such as metal alkoxides, in order to control and to decrease their reactivity [48]. Nonaqueous sol-gel routes were introduced for the same purpose. In fact, the reactivity of the metal oxide precursors is greatly decreased under water exclusion, thus making it easier to control the metal oxide formation [25, 51]. Nonaqueous routes were successfully applied for the synthesis of various metal oxide nanoparticles [19, 43], hybrid materials [36] and also for the growth of metal oxide thin films by atomic layer deposition [5]. Moreover, they gave access to various multimetal and doped oxides.

In spite of the recent progress in nanoparticle research, it is not yet possible to prepare a certain compound on the nanoscale with a desired composition, structure, size and shape, intentionally and in a predicted way. One of the reasons is the fact that it is not yet possible to predict the reactivity of metal complexes in a particular solvent. Moreover, the metal oxide formation is influenced by various additional effects such as intermediate products formed during the reaction, side reactions and catalytic effects of the metal centers, the metal oxide seeds and early formed nanoparticles. Therefore, the synthesis of new materials by nonaqueous sol-gel routes, and other liquid phase approaches, are still based on simple trial-and-error

N. Pinna (✉) · M. Karmaoui · M.-G. Willinger
Department of Chemistry, CICECO, University of Aveiro,
3810-193 Aveiro, Portugal
e-mail: pinna@ua.pt

N. Pinna
World Class University (WCU) program of Chemical
Convergence for Energy & Environment (C2E2), School of
Chemical and Biological Engineering, College of Engineering,
Seoul National University (SNU), Seoul 151-744, Korea
e-mail: pinna@snu.ac.kr

experiments. To go beyond such an approach, a detailed knowledge on the different effects influencing the metal oxide formation must be acquired. One of the ways to progress in this direction is through the generalization of synthesis approaches and by studying the chemical mechanisms taking place during metal oxide formation. Since the most general and versatile approach to metal oxide synthesis is probably the reaction of metal complexes in benzyl alcohol [21, 29, 36, 43] a detailed study of this reaction approach might solve many of the questions enumerated above and perhaps lead to the synthesis of new materials in a more predictable way.

In this article we are going to shortly introduce the “benzyl alcohol route” and its use for the production of multimetal and doped metal oxide nanostructures. In the second part of the manuscript the synthesis and characterization of $ZnAl_2O_4$ complex nanostructures following this method are going to be described.

2 The “benzyl alcohol route”

A particularly attractive reaction approach for the synthesis of crystalline metal oxide nanoparticles is the “benzyl alcohol route”. It is a one pot reaction that, based on the reaction of various metal complexes (e.g. chlorides, alkoxides, acetates, acetylacetones) in benzyl alcohol leads to metal oxide formation in a controlled way. Hereby the latter is acting as solvent, ligand and reactant. The syntheses of titanium, tungsten and vanadium oxides were first reported by Niederberger et al. in 2002 by reacting metal chlorides (i.e. titanium, tungsten and vanadium) with benzyl alcohol between 40 and 120 °C, i.e. well below the boiling point of benzyl alcohol (~ 205 °C) [22, 23]. Just two years later it was reported that the reaction of various metal alkoxides in benzyl alcohol permitted to synthesize various binary and ternary metal oxide nanoparticles [28, 30, 37–39, 41]. In 2009 the number of metal oxides synthesized following this methodology is larger than 50, pointing out the versatility of the approach. The main chemical reactions involved in the metal oxide formation, from the reaction of metal complexes in benzyl alcohol, are the alkylhalide elimination, ester elimination, ether elimination, and the C–C bond formation between benzylic alcohols and alkoxides [19, 25, 29, 43]. It is evident that the ligand plays the most important role in determining the reaction pathway, nevertheless the nature of the metal center can also dramatically influence the chemistry and the characteristics of the final material. The most significant example involves the reaction of metal alkoxides in benzyl alcohol. As a matter of fact, it was demonstrated that the reaction of various metal alkoxides such as $Ti(OiPr)_4$, $Zr(OiPr)_4 \cdot HOiPr$, $Hf(OEt)_4$, $Nb(OEt)_5$ and

$Sn(OiBu)_4$ lead to the elimination of an ether together with the metal oxide formation. However, in the case of $BaTiO_3$ and $NaNbO_3$ the presence of a basic species (Ba and Na alkoxides) was the prerequisite for another mechanism involving a C–C bond formation between alkoxy ligands and benzyl alcohol [13, 25]. Such a mechanism was also demonstrated for metals with high Lewis acidity, such as many rare earth elements (Y, Ce, Gd, Nd, Sm), which can directly catalyze this Guerbet-like reaction [16, 25, 26, 40]. Moreover, the yttrium and some lanthanides (Gd, Nd, Sm) isopropoxides were able to catalyze, in addition to the C–C bond formation between isopropoxy ligands and benzyl alcohol, two additional reactions leading to oxidation of benzyl alcohol to benzoic acid and finally to the formation of oxide-benzoate hybrid nanostructures instead of pure inorganic nanoparticles. The morphological and structural differences between TiO_2 , $BaTiO_3$, $NaNbO_3$ and CeO_2 on one, and the rare earth lamellar organic–inorganic hybrid nanostructures on the other side are also reflected in small, but crucial variations in the organic reaction pathways, pointing out the importance of mechanistic studies in nanomaterial synthesis.

The versatility of nonaqueous routes to oxide nanoparticles was already highlighted in various reviews and will not be further discussed here [21, 26, 27, 29, 43]. In this work we will focus on the peculiar features of the “benzyl alcohol route” that make it possible to synthesize homogeneous ternary, multi-metal and doped oxide nanoparticles.

The different reactivity of metal complexes towards a specific solvent complicates the synthesis of oxides containing two or more metals. In organic solvents (and especially in benzyl alcohol) it is easier to match the reactivity of the metal complexes and of the dopants in comparison to aqueous systems. This is a prerequisite for obtaining single-phase products. Table 1 enumerates the different multimetal oxide nanostructures that have been synthesized in benzyl alcohol. Crystalline titanate, niobate, aluminate nanostructures and other important multimetal oxides are readily obtained at temperatures varying from 180 to 275 °C. From Table 1 it appears evident that various metal complexes can be employed ranging from simple inorganic (e.g. chlorides and nitrates) to metal organic (e.g. acetates, acetylacetones and alkoxydes) complexes. For example, Xiao et al. [54] showed that the reaction of $Zn(NO_3)_2 \cdot H_2O$ and NH_4VO_3 in benzyl alcohol leads to ZnV_2O_4 hollow spheres having a complex nanostructure, highlighting that simple and inexpensive precursors can also be used (Fig. 1 a, b). The reaction of calcium methoxide and aluminum isopropoxide in benzyl alcohol lead to flower like complex nanostructures of $CaAl_4O_7$ consisting of thin platelets or needles as shown in Fig. 1c [17]. About 5–10 nm $YNbO_4$ nanoparticles (Fig. 1d) can be synthesized from $Y(acac)_3 \cdot xH_2O$ and $NbCl_5$ [56]. Five nanometers

Table 1 Ternary and multi metal oxide nanoparticles synthesized in benzyl alcohol

Metal oxide	Precursors	Shape	Ref.
Antimony tin oxide	$\text{SnCl}_4 + \text{SbCl}_3$	Spherical	[49]
BaAl_2O_4	$\text{Ba} + \text{Al(OiPr)}_3$	Flower like	[17]
BaTiO_3	$\text{Ba} + \text{Ti(OiPr)}_4$	Spherical	[3, 28, 30]
BaZrO_3	$\text{Ba} + \text{Zr(OiPr)}_4 \cdot \text{HOiPr}$	Slightly elongated	[30]
$(\text{Ba},\text{Sr})\text{TiO}_3$	$\text{Ba} + \text{Sr} + \text{Ti(OiPr)}_4$	Spherical	[28]
CaAl_4O_7	$\text{Ca(OMe)}_2 + \text{Al(OiPr)}_3$	Flower like	[17]
CdIn_2O_4	$\text{Cd(ac)}_2 + \text{In(OiPr)}_3$	Spherical	[4, 52]
InNbO_4	$\text{In(acac)}_3 + \text{NbCl}_5$	Spherical	[55, 56]
Indium tin oxide	$\text{In(acac)}_3 + \text{Sn(OtBu)}_4$	Spherical	[1, 2]
$\text{La}_{1-x}\text{A}_x\text{MnO}_3$ ($\text{A} = \text{Ca, Sr, Ba}$)	Various	—	[50]
LiNbO_3	$\text{Li} + \text{Nb(OEt)}_5$	—	[30]
MnNb_2O_6	$\text{Mn(acac)}_3 + \text{NbCl}_5$	—	[56]
NaNbO_3	$\text{Na} + \text{Nb(OEt)}_5$	Spherical	[14]
NaTaO_3	$\text{Na} + \text{Ta(OEt)}_5$	—	[14]
SrAl_4O_7	$\text{Sr} + \text{Al(OiPr)}_3$	Flower like	[17]
SrTiO_3	$\text{Sr} + \text{Ti(OiPr)}_4$	Spherical	[28]
YNbO_4	$\text{Y(acac)}_3 \cdot x\text{H}_2\text{O} + \text{NbCl}_5$	Spherical	[56]
ZnAl_2O_4	$\text{Zn(ac)}_2 + \text{Al(OiPr)}_3$	Spherical	This work
ZnV_2O_4	$\text{Zn}(\text{NO}_3)_2 \cdot \text{H}_2\text{O} + \text{NH}_4\text{VO}_3$	Hollow spheres	[54]

ac = acetate, acac = acetylacetone

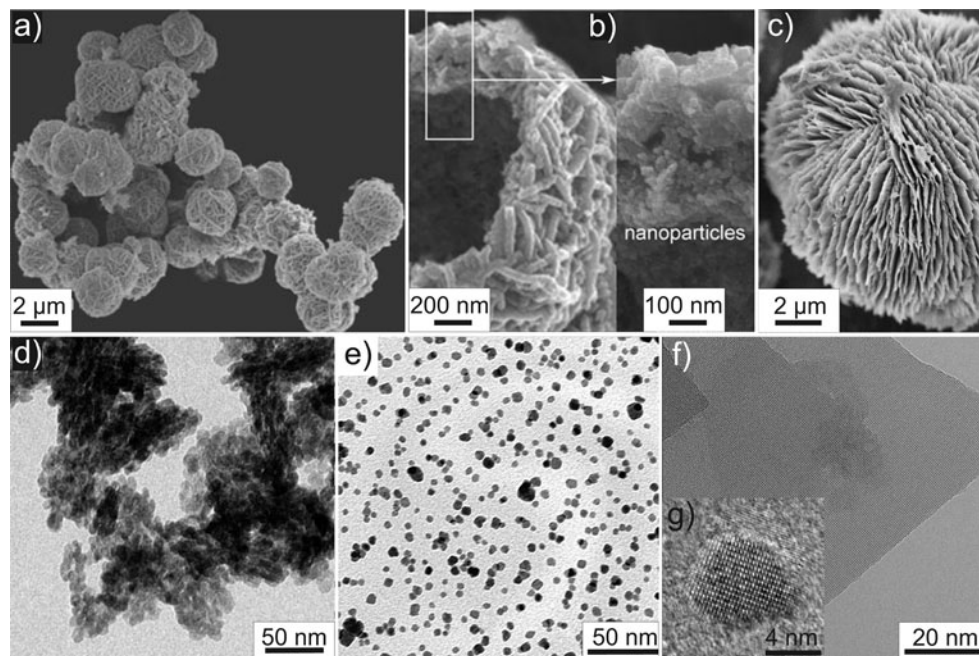


Fig. 1 **a, b** SEM images of ZnV_2O_4 hollow spheres reproduced with permission from reference [54]. **c** SEM of CaAl_4O_7 nanostructures [17]. **d** TEM of YNbO_4 nanoparticles reproduced with permission from reference [56]. **e** TEM of indium tin oxide nanoparticles

Indium tin oxide nanoparticles (Fig. 1e) are obtained from In(acac)_3 and Sn(OtBu)_4 . These last examples highlight the fact that in order to match the reactivity of the metal

reproduced with permission from reference [2]. **f** HRTEM of the ending of a CaAl_4O_7 nanostructure shown in c) [17]. **g** HRTEM of a $(\text{Ba},\text{Sr})\text{TiO}_3$ nanoparticle [28]

complexes in benzyl alcohol it is often necessary to employ different ligands for each metal center. As a typical example, solid solution of indium tin oxide nanoparticles could

Table 2 Doped metal oxide nanoparticles synthesized in benzyl alcohol

Metal oxide	Precursors	Shape	Ref.
Mn-/Cr-doped HfO ₂	Hf(OtBu) ₄ + Mn(acac) ₃ , Mn(acac) ₂ , Mn(ac) ₂ or Cr(acac) ₃	Spherical	[47]
Co-/Fe-doped TiO ₂	Co(acac) ₂ , Fe(acac) ₃ , Ti(OiPr) ₄ , TiCl ₄	Spherical or well-faceted	[10]
Mn-/Co-doped ZnO	Zn(ac) ₂ + Mn(oleate) ₂ or Co(ac) ₂	Nanorods and Nanowires	[6]
Mn-/Co-doped ZnO	Zn(acac) ₂ ·xH ₂ O + Mn(acac) ₂ or Co(acac) ₂	Nanorods	[11]
Eu-doped ZrO ₂	Zr(OiPr) ₄ ·HOiPr + Eu(acac) ₃ ·xH ₂ O	Spherical	[31]
Mn-/Cr-doped ZrO ₂	Zr(OiPr) ₄ ·HOiPr + Mn(acac) ₃ , Mn(ac) ₂ or Cr(acac) ₃	Spherical	[7, 47]

ac = acetate, acac = acetylacetone

not be obtained using In(III) alkoxide instead of In(acac)₃ because in this case, the different reactivity of the two metal complexes does not permit the formation of a solid solution [20, 42]. The particles size and shape greatly differ from one system to another, but within a particular system the materials are rather monodisperse.

Finally, the high crystallinity of the as synthesized multimetal oxide nanostructures is demonstrated by the Fig. 1f, g. They show, respectively, HRTEM images of CaAl₄O₇ platelets that build up the flower like structures shown in Fig. 1c and a 6 nm sized (Ba,Sr)TiO₃ nanoparticle.

Nonaqueous reaction conditions seem to be particularly suitable for doping of binary metal oxide nanoparticles as well (Table 2). The most studied systems are the non-magnetic binary oxides (e.g. ZnO, ZrO₂, HfO₂) doped with magnetic impurities (e.g. Co, Mn) for application in e.g. spintronic. The synthesis approach proved to be rather robust also in this case and led to the homogeneous doping of various binary oxides with magnetic ions even at relatively high dopant concentration. The largest effective doping concentration (17%) was obtained for HfO₂ doped with Mn from Mn(acac)₃. In almost all these cases a detailed characterization of the doping homogeneity and behavior was performed in order to correlate the structural, doping and magnetic properties [6, 47].

3 ZnAl₂O₄ nanostructures by oriented attachment

Zinc aluminate, a catalyst and catalyst support, can be obtained at the nanoscale by soft chemistry routes and by making use of the Kirkendall effect, allowing the formation of well defined nanotubes starting from an anodized aluminum oxide template impregnated with zinc oxide, or from zinc oxide nanowires coated with alumina [12, 53]. The solvothermal reaction ($T = 250$ °C) of Zn(ac)₂ and Al(OiPr)₃ in benzyl alcohol for two days leads to the formation of ZnAl₂O₄ nanostructures. The X-ray diffraction pattern (XRD) is typical for the spinel ZnAl₂O₄ structure (Fig. 2). The width of the reflections speak for a nanostructured material with an average crystallite size of 10 nm as estimated using the Scherrer equation. The TEM

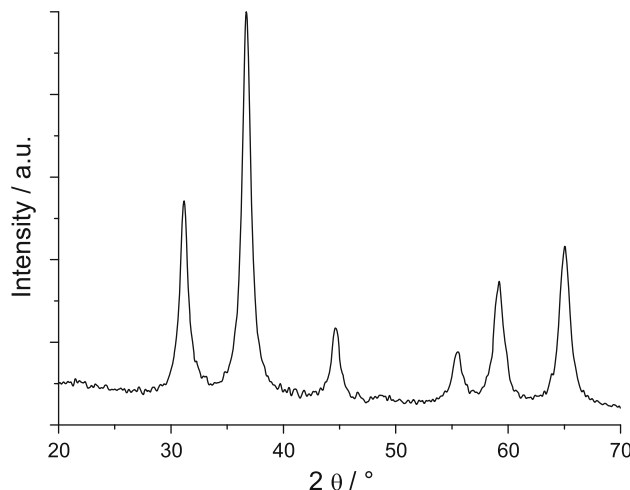


Fig. 2 XRD pattern of ZnAl₂O₄ nanocrystals

observation reveals that the as synthesizes ZnAl₂O₄ forms flower-like nanostructures of around 30 nm in size (Fig. 3a). High resolution images recorded from these nanostructures reveal that they are constituted of well defined 5–6 nm primary particles (Fig. 3b). The size of these primary particles is therefore slightly smaller than the crystalline size extracted from XRD measurements. Analysis of the lattice fringes reveals that the planes of neighboring nanoparticles coincide. Furthermore, the power spectrum of the whole image resembles that of a single crystal (inset of Fig. 3b; the zone axis is [111]). This observation indicates that the flower-like aggregates are formed by an oriented attachment crystallization mechanism. Oriented attachment involves the interaction of adjacent particles and their fusion, leading to nanostructured aggregates that appear as single crystals which often contain defects at the interface where the primary particles fuse. This mechanism was firstly reported by Penn and Banfield on the study of aggregation of anatase nanoparticles under hydrothermal conditions [33–35]. After these first reports many other have followed for many other systems, mostly for metal oxide nanoparticles (cf. e.g. [44–46, 57]). Such a non-classical crystallization mechanism was recently reviewed by Coelfen et al. [8, 24].

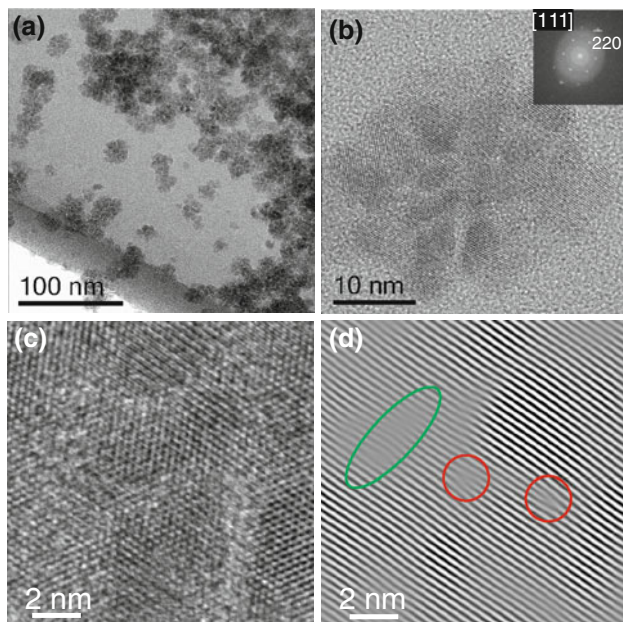


Fig. 3 TEM images of the ZnAl_2O_4 nanostructures. **a** Overview, **b** high resolution images. Inset power spectrum of **b** the zone axis is the [111]. **c** detail of the HRTEM image in **b** used for the Fourier analysis **d** using the $\bar{2}20$ reflection. Red circles show dislocations and the green circle- a zone of non perfect orientational matching between planes of two attached nanoparticles. (Color figure online)

In order to verify this hypothesis, Fourier filtered images using the $\bar{2}20$ reflection of the power spectrum shown in the inset of Fig. 3b were calculated. For better clarity only a portion of the image is shown. Figure 3c and d present a detail of the HRTEM image in b and the corresponding filtered image using the $\bar{2}20$ reflection. In the FFT filtered image, dislocations (red circles) and zones where particles are not perfectly attached (e.g. green ellipsoid) are easier to see. These defects are typical for the oriented attachment crystallization mechanism similarly to the case of tungstite nanoplatelets [46].

4 Conclusions

In this article the versatility and the potential of the “benzyl alcohol route” for the synthesis of multimetal and doped metal oxides were highlighted. Among the examples cited some of the materials are not accessible by other solution synthesis but only by solid state reactions. The second part of the manuscript described the synthesis and characterization of 5–6 nm ZnAl_2O_4 nanoparticles, which form flower-like aggregates by the oriented attachment crystallization mechanism.

This article brings further confirmation on the fact that the “benzyl alcohol route” is the most general, versatile

and widely applicable approach for the synthesis of crystalline multimetal and doped metal oxide nanostructures in solution and this at relatively low temperature. Finally, additional studies are still needed on the further generalization of the “benzyl alcohol route” and on the growth mechanisms. Indeed, they might permit to go beyond the trial-and-error approach for the synthesis of new materials.

Acknowledgements This work was partially supported by the European Network of Excellence FAME, the WCU (World Class University) program through the Korea Science and Engineering Foundation funded by the Ministry of Education, Science and Technology (400-2008-0230), and FCT Project No. (PTDC/CTM/65667/2006)

References

- Ba J, Feldhoff A, Fattakhova-Rohlfing D, Wark M, Antonietti M, Niederberger M (2007) Crystallization of indium tin oxide nanoparticles: from cooperative behavior to individuality. *Small* 3:310–317. doi:[10.1002/smll.200600425](https://doi.org/10.1002/smll.200600425)
- Ba JH, Fattakhova-Rohlfing D, Feldhoff A, Brezesinski T, Djerdj I, Wark M, Niederberger M (2006) Nonaqueous synthesis of uniform indium tin oxide nanocrystals and their electrical conductivity in dependence of the tin oxide concentration. *Chem Mater* 18:2848–2854. doi:[10.1021/cm060548q](https://doi.org/10.1021/cm060548q)
- Bilecka I, Djerdj I, Niederberger M (2008) One-minute synthesis of crystalline binary and ternary metal oxide nanoparticles. *Chem Commun* 886–888. doi:[10.1039/b717334b](https://doi.org/10.1039/b717334b)
- Cao M, Wang Y, Chen T, Antonietti M, Niederberger M (2008) A highly sensitive and fast-responding ethanol sensor based on CdIn_2O_4 nanocrystals synthesized by a nonaqueous sol-gel route. *Chem Mater* 20:5781–5786. doi:[10.1021/cm800794y](https://doi.org/10.1021/cm800794y)
- Clavel G, Rauwel E, Willinger MG, Pinna N (2009) Nonaqueous sol-gel routes applied to atomic layer deposition of oxides. *J Mater Chem* 19:454–462. doi:[10.1039/b806215c](https://doi.org/10.1039/b806215c)
- Clavel G, Willinger MG, Zitoun D, Pinna N (2007) Solvent dependent shape and magnetic properties of doped ZnO nanostructures. *Adv Funct Mater* 17:3159–3169. doi:[10.1002/adfm.200601142](https://doi.org/10.1002/adfm.200601142)
- Clavel G, Willinger MG, Zitoun D, Pinna N (2008) Manganese-doped zirconia nanocrystals. *Eur J Inorg Chem* 2008(6):863–868. doi:[10.1002/ejic.200700977](https://doi.org/10.1002/ejic.200700977)
- Coelfen H, Antonietti M (2008) Mesocrystals and nonclassical crystallization. John Wiley & Sons Ltd., Chichester, England
- Cushing BL, Kolesnichenko VL, O'Connor CJ (2004) Recent advances in the liquid-phase syntheses of inorganic nanoparticles. *Chem Rev* 104:3893–3946. doi:[10.1021/cr030027b](https://doi.org/10.1021/cr030027b)
- Djerdj I, Arcon D, Jaglicic Z, Niederberger M (2008) Nonaqueous synthesis of metal oxide nanoparticles: short review and doped titanium dioxide as case study for the preparation of transition-metal doped oxide nanoparticles. *J Solid State Chem* 181:1574–1584. doi:[10.1016/j.jssc.2008.04.016](https://doi.org/10.1016/j.jssc.2008.04.016)
- Djerdj I, Garnweiter G, Arcon DMP, Zvonko J, Niederberger M (2008) Diluted magnetic semiconductors: Mn/Co-doped ZnO nanorods as case study. *J Mater Chem* 18:5208–5217. doi:[10.1039/b808361d](https://doi.org/10.1039/b808361d)
- Fan HJ, Knez M, Scholz R, Nielsch K, Pippel E, Hesse D, Zacharias M, Goesele U (2006) Monocrystalline spinel nanotube fabrication based on the kirkendall effect. *Nature Mater* 5:627–631. doi:[10.1038/nmat1673](https://doi.org/10.1038/nmat1673)

13. Garnweitner G (2005) Nonaqueous synthesis of transition-metal oxide nanoparticles and their formation mechanism. Ph.D. thesis, University of Potsdam. <http://www.opus.kobv.de/ubp/volltexte/2005/589/>
14. Garnweitner G, Niederberger M (2006) Nonaqueous and surfactant-free synthesis routes to metal oxide nanoparticles. *J Am Ceram Soc* 89:1801–1808. doi:[10.1111/j.1551-2916.2006.01005.x](https://doi.org/10.1111/j.1551-2916.2006.01005.x)
15. Jun YW, Choi JS, Cheon J (2006) Shape control of semiconductor and metal oxide nanocrystals through nonhydrolytic colloidal routes. *Angew. Chem Int Ed* 45:3414–3439. doi:[10.1002/anie.200503821](https://doi.org/10.1002/anie.200503821)
16. Karnaoui M, Ferreira RAS, Mane AT, Carlos LD, Pinna N (2006) Lanthanide-based lamellar nanohybrids: Synthesis, structural characterization, and optical properties. *Chem Mater* 18:4493–4499. doi:[10.1021/cm0607051](https://doi.org/10.1021/cm0607051)
17. Karnaoui M, Willinger MG, Mafra L, Hernrich T, Pinna N (2009) A general nonaqueous route to crystalline alkaline earth aluminates nanostructures. *Nanoscale*. doi:[10.1039/b9nr00164f](https://doi.org/10.1039/b9nr00164f)
18. Livage J, Henry M, Sanchez C (1988) Sol-gel chemistry of transition metal oxides. *Prog Solid State Chem* 18:259–341. doi:[10.1016/0079-6786\(88\)90005-2](https://doi.org/10.1016/0079-6786(88)90005-2)
19. Mutin PH, Vioux A (2009) Nonhydrolytic processing of oxide-based materials: Simple routes to control homogeneity, morphology, and nanostructure. *Chem Mater* 21:582–596. doi:[10.1021/cm802348c](https://doi.org/10.1021/cm802348c)
20. Neri G, Bonavita A, Rizzo G, Galvagno S, Pinna N, Niederberger M, Capone S, Siciliano P (2007) Towards enhanced performances in gas sensing: SnO₂ based nanocrystalline oxides application. *Sens Actuators B* 122:564–571. doi:[10.1016/j.snb.2006.07.006](https://doi.org/10.1016/j.snb.2006.07.006)
21. Niederberger M (2007) Nonaqueous sol-gel routes to metal oxide nanoparticles. *Acc Chem Res* 40:793–800. doi:[10.1021/ar60035e](https://doi.org/10.1021/ar60035e)
22. Niederberger M, Bartl MH, Stucky GD (2002) Benzyl alcohol and titanium tetrachloride: a versatile reaction system for the nonaqueous and low-temperature preparation of crystalline and luminescent titania nanoparticles. *Chem Mater* 14:4364–4370. doi:[10.1021/cm021203k](https://doi.org/10.1021/cm021203k)
23. Niederberger M, Bartl MH, Stucky GD (2002) Benzyl alcohol and transition metal chlorides as a versatile reaction system for the nonaqueous and low-temperature synthesis of crystalline nano-objects with controlled dimensionality. *J Am Chem Soc* 124:13642–13643. doi:[10.1021/ja027115i](https://doi.org/10.1021/ja027115i)
24. Niederberger M, Coelfen H (2006) Oriented attachment and mesocrystals: non-classical crystallization mechanisms based on nanoparticle assembly. *Phys Chem Chem Phys* 8:3271–3287. doi:[10.1039/b604589h](https://doi.org/10.1039/b604589h)
25. Niederberger M, Garnweitner G (2006) Organic reaction pathways in the nonaqueous synthesis of metal oxide nanoparticles. *Chem Eur J* 12:7282–7302. doi:[10.1002/chem.200600313](https://doi.org/10.1002/chem.200600313)
26. Niederberger M, Garnweitner G, Ba J, Polleux J, Pinna N (2007) Nonaqueous synthesis, assembly and formation mechanisms of metal oxide nanocrystals. *Int J Nanotechnol* 4:263–281. doi:[10.1504/IJNT.2007.013473](https://doi.org/10.1504/IJNT.2007.013473)
27. Niederberger M, Garnweitner G, Buha J, Polleux J, Ba J, Pinna N (2006) Nonaqueous synthesis of metal oxide nanoparticles: review and indium oxide as case study for the dependence of particle morphology on precursors and solvents. *J Sol-Gel Sci Technol* 40:259–266. doi:[10.1007/s10971-006-6668-8](https://doi.org/10.1007/s10971-006-6668-8)
28. Niederberger M, Garnweitner G, Pinna N, Antonietti M (2004) Nonaqueous and halide-free route to crystalline BaTiO₃, SrTiO₃, and (Ba,Sr)TiO₃ nanoparticles via a mechanism involving c–c bond formation. *J Am Chem Soc* 126:9120–9126. doi:[10.1021/ja0494959](https://doi.org/10.1021/ja0494959)
29. Niederberger M, Pinna N (2009) Metal oxide nanoparticles in organic solvents: synthesis, formation, assembly and application. Springer ISBN:978-1-84882-670-0
30. Niederberger M, Pinna N, Polleux J, Antonietti M (2004) A general soft chemistry route to perovskites and related materials: synthesis of BaTiO₃, BaZrO₃ and LiNbO₃ nanoparticles. *Angew Chem Int Ed* 43:2270–2273. doi:[10.1002/anie.200353300](https://doi.org/10.1002/anie.200353300)
31. Ninjabdar T, Garnweitner G, Börger A, Goldenberg LM, Sakhno OV, Stumpe J (2009) Synthesis of luminescent ZrO₂:Eu³⁺ nanoparticles and their holographic sub-micrometer patterning in polymer composites. *Adv Funct Mater* 19:1819–1825. doi:[10.1002/adfm.200801835](https://doi.org/10.1002/adfm.200801835)
32. Park J, Joo J, Kwon SG, Jang Y, Hyeon T (2007) Synthesis of monodisperse spherical nanocrystals. *Angew Chem Int Ed* 46:4630–4660. doi:[10.1002/anie.200603148](https://doi.org/10.1002/anie.200603148)
33. Penn RL, Banfield JF (1998) Imperfect oriented attachment: dislocation generation in defect-free nanocrystals. *Science* 281:969–971. doi:[10.1126/science.281.5379.969](https://doi.org/10.1126/science.281.5379.969)
34. Penn RL, Banfield JF (1998) Oriented attachment and growth, twinning, polytypism, and formation of metastable phases: insights from nanocrystalline TiO₂. *Am Mineral* 83:1077–1082
35. Penn RL, Banfield JF (1999) Morphology development and crystal growth in nanocrystalline aggregates under hydrothermal conditions: insights from titania. *Geochim Cosmochim Acta* 63:1549–1557. doi:[10.1016/S0016-7037\(99\)00037-X](https://doi.org/10.1016/S0016-7037(99)00037-X)
36. Pinna N (2007) The “benzyl alcohol route”: an elegant approach towards organic–inorganic hybrid nanomaterials. *J Mater Chem* 17:2769–2774. doi:[10.1039/b702854g](https://doi.org/10.1039/b702854g)
37. Pinna N, Antonietti M, Niederberger M (2004) A novel nonaqueous route to V₂O₃ and Nb₂O₅ nanocrystals. *Colloids Surf A* 250:211–213. doi:[10.1016/j.colsurfa.2004.04.078](https://doi.org/10.1016/j.colsurfa.2004.04.078)
38. Pinna N, Bonavita, A, Neri, G, Capone S, Siciliano P, Niederberger M (2004) Nonaqueous synthesis of high-purity indium and tin oxide nanocrystals and their application as gas sensors. In: Proceedings of the IEEE sensors, pp 192–195
39. Pinna N, Garnweitner G, Antonietti M, Niederberger M (2004) Non-aqueous synthesis of high-purity metal oxide nanopowders using an ether elimination process. *Adv Mater* 16:2196–2200. doi:[10.1002/adma.200400460](https://doi.org/10.1002/adma.200400460)
40. Pinna N, Garnweitner G, Beato P, Niederberger M, Antonietti M (2005) Synthesis of yttria-based crystalline and lamellar nanostructures and their formation mechanism. *Small* 1:112–121. doi:[10.1002/smll.200400014](https://doi.org/10.1002/smll.200400014)
41. Pinna N, Neri G, Antonietti M, Niederberger M (2004) Non-aqueous synthesis of nanocrystalline semiconducting metal oxides for gas sensing. *Angew Chem Int Ed* 43:4345–4349. doi:[10.1002/anie.200460610](https://doi.org/10.1002/anie.200460610)
42. Pinna N, Niederberger M Unpublished
43. Pinna N, Niederberger M (2008) Surfactant-free nonaqueous synthesis of metal oxide nanostructures. *Angew Chem Int Ed* 47:5292–5304. doi:[10.1002/anie.200704541](https://doi.org/10.1002/anie.200704541)
44. Polleux J, Pinna N, Antonietti M, Hess C, Wild U, Schlogl R, Niederberger M (2005) Ligand functionality as a versatile tool to control the assembly behavior of preformed titania nanocrystals. *Chem Eur J* 11:3541–3551. doi:[10.1002/chem.200401050](https://doi.org/10.1002/chem.200401050)
45. Polleux J, Pinna N, Antonietti M, Niederberger M (2004) Ligand-directed assembly of preformed titania nanocrystals into highly anisotropic nanostructures. *Adv Mater* 16:436–439. doi:[10.1002/adma.200306251](https://doi.org/10.1002/adma.200306251)
46. Polleux J, Pinna N, Antonietti M, Niederberger M (2005) Growth and assembly of crystalline tungsten oxide nanostructures assisted by bioligation. *J Am Chem Soc* 127:15595–15601. doi:[10.1021/ja0544915](https://doi.org/10.1021/ja0544915)
47. Pucci A, Clavel G, Willinger MG, Zitoun D, Pinna N (2009) Transition metal doped ZrO₂ and HfO₂ nanocrystals. *J Phys Chem C* 113:12048–12058. doi:[10.1021/jp9029375](https://doi.org/10.1021/jp9029375)
48. Sanchez C, Livage J, Henry M, Babonneau F (1988) Chemical modification of alkoxide precursors. *J Non-Cryst Solids* 100:65–76. doi:[10.1016/0022-3093\(88\)90007-5](https://doi.org/10.1016/0022-3093(88)90007-5)

49. da Silva RO, Conti TG, de Moura AF, Stroppa DG, Freitas LCG, Ribeiro C, Camargo ER, Longo E, Leite ER (2009) Antimony-doped tin oxide nanocrystals:synthesis and solubility behavior in organic solvents. *Chem Phys Chem* 10:841–846. doi:[10.1002/cphc.200800764](https://doi.org/10.1002/cphc.200800764)
50. Vazquez-Vazquez C, Lopez-Quintela MA (2006) Solvothermal synthesis and characterisation of $\text{La}_{1-x}\text{A}_x\text{MnO}_3$ nanoparticles. *J Solid State Chem* 179:3229–3237. doi:[10.1016/j.jssc.2006.06.021](https://doi.org/10.1016/j.jssc.2006.06.021)
51. Vioux A (1997) Nonhydrolytic sol–gel routes to oxides. *Chem Mater* 9:2292–2299. doi:[10.1021/cm970322a](https://doi.org/10.1021/cm970322a)
52. Wang Y, Chen T, Mu Q, Wang G (2009) A nonaqueous sol–gel route to synthesize CdIn_2O_4 nanoparticles for the improvement of formaldehyde-sensing performance. *Scripta Mater* 61:935–938. doi:[10.1016/j.scriptamat.2009.07.029](https://doi.org/10.1016/j.scriptamat.2009.07.029)
53. Wang Y, Wu K (2005) As a whole:Crystalline zinc aluminate nanotube array-nanonet. *J Am Chem Soc* 127:9686–9687. doi:[10.1021/ja0505402](https://doi.org/10.1021/ja0505402)
54. Xiao L, Zhao Y, Yin J, Zhang L (2009) Clewlike ZnV_2O_4 hollow spheres:Nonaqueous sol–gel synthesis, formation mechanism, and lithium storage properties. *Chem Eur J* 15:9442–9450. doi:[10.1002/chem.200901328](https://doi.org/10.1002/chem.200901328)
55. Zhang L, Djerdj I, Cao M, Antonietti M, Niederberger M (2007) Nonaqueous sol–gel synthesis of nanocrystalline InNbO_4 visible light photocatalyst. *Adv Mater* 19:2083–2086. doi:[10.1002/adma.200700027](https://doi.org/10.1002/adma.200700027)
56. Zhang L, Garnweinertner G, Djerdj I, Antonietti M, Niederberger M (2008) Generalized nonaqueous sol–gel synthesis of different transition metal niobate nanocrystals and analysis of the growth mechanism. *Chem Asian J* 3:746–752. doi:[10.1002/asia.200700318](https://doi.org/10.1002/asia.200700318)
57. Zitoun D, Pinna N, Frolet N, Belin C (2005) Single crystal manganese oxide multipods by oriented attachment. *J Am Chem Soc* 127:15034–15035. doi:[10.1021/ja0555926](https://doi.org/10.1021/ja0555926)